

## Studies on *Alismatis Rhizoma*. III.<sup>1)</sup> Stereostructures of New Protostane-Type Triterpenes, Alisols H, I, J-23-Acetate, K-23-Acetate, L-23-Acetate, M-23-Acetate, and N-23-Acetate, from the Dried Rhizome of *Alisma orientale*

Masayuki YOSHIKAWA,<sup>\*,a</sup> Norimichi TOMOHIRO,<sup>b</sup> Toshiyuki MURAKAMI,<sup>a</sup> Akira IKEBATA,<sup>a</sup>  
Hisashi MATSUDA,<sup>a</sup> Hideaki MATSUDA,<sup>b</sup> and Michinori KUBO<sup>b</sup>

*Kyoto Pharmaceutical University,<sup>a</sup> 5 Nakauchi-cho, Misasagi, Yamashina-ku, Kyoto 607-8414, Japan and Faculty of  
Pharmaceutical Sciences, Kinki University,<sup>b</sup> 3-4-1, Kowakae, Higashiosaka, Osaka 577-0818, Japan.*

Received November 24, 1998; accepted January 11, 1999

**New protostane-type triterpenes termed alisols H, I, J-23-acetate, K-23-acetate, L-23-acetate, M-23-acetate, and N-23-acetate were isolated from *Alismatis Rhizoma*, the rhizome of *Alisma orientale* JUZEJ. Their stereostructures were determined on the basis of physicochemical evidence.**

**Key words** alisol H; *Alismatis Rhizoma*; *Alisma orientale*; protostane-type triterpene; alisol N-23-acetate

We previously reported that the methanolic extract of *Alismatis Rhizoma* showed inhibitory activities against experimental models of type I, II, III, and IV allergies: that is, 48 h homologous passive cutaneous anaphylaxis in rats, reversed cutaneous anaphylaxis in rats, direct passive Arthus reaction in rats, and picryl chloride-induced contact dermatitis in mice.<sup>2)</sup> As the constituents responsible for anti-allergic activity of this natural medicine, four protostane-type triterpenes, alisols A (**1**)<sup>3)</sup> and B (**3**)<sup>3)</sup> and their monoacetates (**2**, **4**)<sup>3)</sup> and two sesquiterpenes, alismol<sup>4)</sup> and alismoxide,<sup>4)</sup> were characterized.<sup>2)</sup> The methanolic extract of *Alismatis Rhizoma* was also found to exhibit anti-complementary activities and to inhibit complement-induced hemolysis and hypotonic shock-induced hemolysis. Furthermore, we have found that four principal triterpene constituents (**1**—**4**) inhibited the complement-induced hemolysis, while two sesquiterpenes, alismol and alismoxide, were ineffective.<sup>1)</sup>

As a continuing part of our studies on *Alismatis Rhizoma*, we have isolated seven new protostane-type triterpenes called alisols H (**10**), I (**11**), J-23-acetate (**12**), K-23-acetate (**13**), L-23-acetate (**14**), M-23-acetate (**15**), and N-23-acetate (**16**) from the methanolic extract with anti-allergic and anti-complementary activities. In this paper, we elucidate the structure of these new protostane-type triterpenes (**10**—**16**).

The methanolic extract of *Alismatis Rhizoma* was partitioned into a mixture of ethyl acetate and water to furnish the ethyl acetate-soluble portion and the water-soluble portion as described in previous papers.<sup>1,2)</sup> The ethyl acetate-soluble portion was subjected to silica gel and octadecyl silica (ODS) column and finally HPLC to give alisols H (**10**), I (**11**), J-23-acetate (**12**), K-23-acetate (**13**), L-23-acetate (**14**), M-23-acetate (**15**), and N-23-acetate (**16**) together with **1**—**4**, alismol, alismoxide, 11-deoxyalisols B (**5**) and B-23-acetate (**6**),<sup>5)</sup> 11-deoxyalisols C (**7**)<sup>6)</sup> and C monoacetate (**8**),<sup>7)</sup> and 11-deoxyalisol D (**9**).<sup>7)</sup>

Alisol H (**10**) showed absorption bands at 3481, 1705, 1700, and 1665 cm<sup>-1</sup> assignable to hydroxyl, ketone, and enone functions in its IR spectrum. The UV spectrum of **10** showed absorption maximum at 243 nm (log  $\epsilon$  3.8) suggestive of an enone function. In the negative-ion FAB-MS of **10**, a quasimolecular ion peak was observed at  $m/z$  469 (M-

H)<sup>-</sup>, while its positive-ion FAB-MS showed quasimolecular ion peaks at  $m/z$  471 (M+H)<sup>+</sup> and 493 (M+Na)<sup>+</sup>. High-resolution MS analysis of the quasimolecular ion peak (M+H)<sup>+</sup> in the positive-ion FAB-MS revealed the molecular formula of **10** to be C<sub>30</sub>H<sub>46</sub>O<sub>4</sub>.

The <sup>1</sup>H-NMR (CDCl<sub>3</sub>) and <sup>13</sup>C-NMR (Table 1) spectra of **10**, which were assigned with the aid of various NMR analytical methods,<sup>8)</sup> showed signals assignable to two isolated methylenes [ $\delta$  1.80, 2.44 (both d,  $J=19.5$  Hz, 15-H<sub>2</sub>), 2.52, 2.54 (both d,  $J=20.3$  Hz, 24-H<sub>2</sub>)] and two methylenes [ $\delta$  2.30, 2.64 (both m, 2-H<sub>2</sub>), 2.66, 2.98 (both m, 22-H<sub>2</sub>)] adjacent to a ketocarbonyl group together with seven tertiary methyls, a secondary methyl, three ketocarbonyls, and a tetrasubstituted olefin. The plane structure of **10** including the positions of the three ketocarbonyl groups and an olefin function was clarified by a heteronuclear multiple bond correlation (HMBC) experiment on **10**, which showed long-range correlations between the following protons and carbons: 3-C and 2-H<sub>2</sub>, 28-H<sub>3</sub>, 29-H<sub>3</sub>; 16-C and 15-H<sub>2</sub>; 23-C and 22-H<sub>2</sub>, 24-H<sub>2</sub>; 13-C and 18-H<sub>3</sub>; 17-C and 20-H, 21-H<sub>3</sub>, 22-H<sub>2</sub> (Fig. 1 A). The protostane-type stereostructure of **10** was confirmed by a nuclear Overhauser effect spectroscopy (NOESY) spectrum as shown in Fig. 2 a. Furthermore, the carbon signals in the <sup>13</sup>C-NMR spectrum of **10** were found to be superimposable on those of 11-deoxyalisol C (**7**),<sup>6)</sup> except for the signals due to the side chain moiety (C-22—27), so that the structure of alisol H (**10**) was determined as shown.

The IR spectrum of alisol I (**11**) showed an absorption band at 1705 cm<sup>-1</sup> ascribable to the ketone function. In the electron impact-mass spectrum (EI-MS) of **11**, a molecular ion peak was observed at  $m/z$  454 (M<sup>+</sup>) and the molecular formula C<sub>30</sub>H<sub>46</sub>O<sub>3</sub> was determined by high-resolution MS measurement. The <sup>1</sup>H-NMR (CDCl<sub>3</sub>) and <sup>13</sup>C-NMR (Table 1) spectra of **11**<sup>8)</sup> showed signals assignable to three methines bearing an oxygen function [ $\delta$  4.47 (dd-like, 16-H), 3.53 (ddd,  $J=2.1, 7.9, 12.2$  Hz, 23-H), 2.71 (d,  $J=7.9$  Hz, 24-H)] together with seven tertiary methyls, a secondary methyl, a ketocarbonyl, and a tetrasubstituted olefin. Comparison of the <sup>1</sup>H- and <sup>13</sup>C-NMR spectra for **11** with those for alisol F<sup>9)</sup> and 16,23-oxidoalisol B<sup>7)</sup> allowed us to presume the presence of the 24,25-oxide and 16,23-oxide rings in the protostane-

\* To whom correspondence should be addressed.

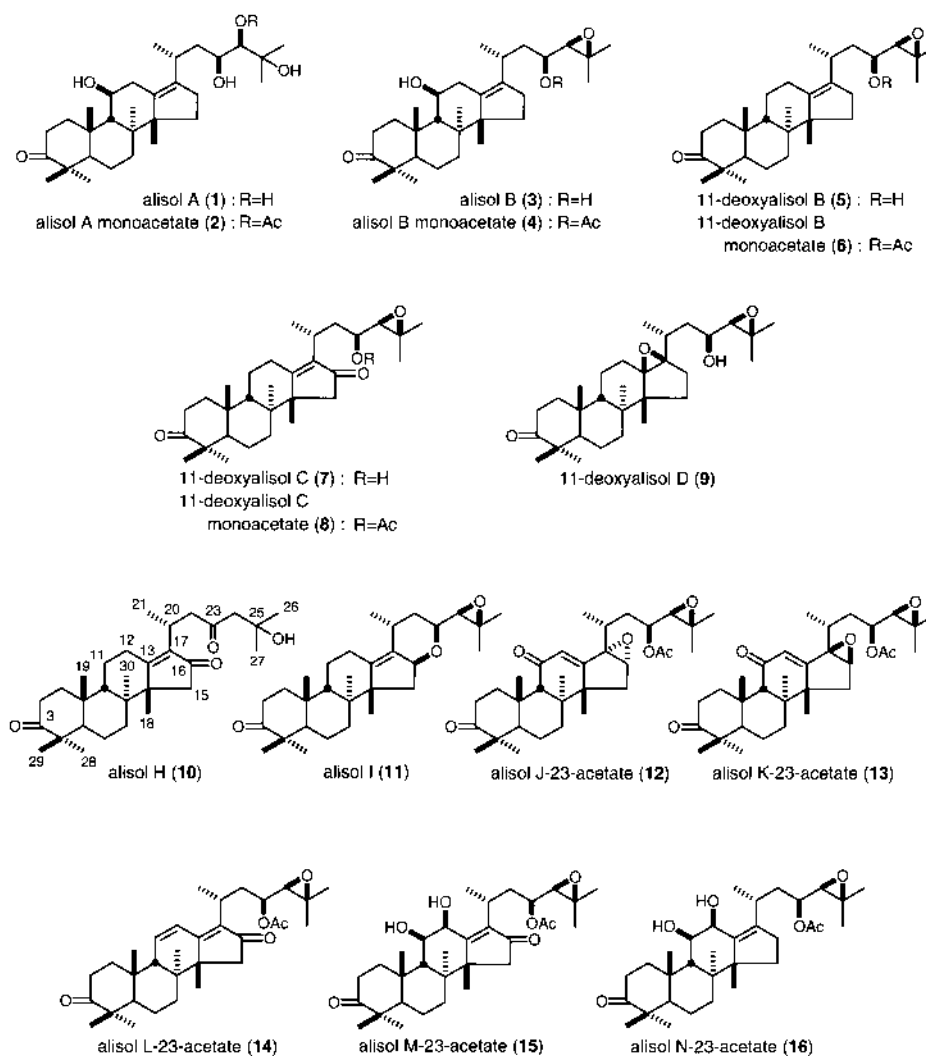


Chart 1

type triterpene structure of **11**. The positions of the ketocarbonyl and tetrasubstituted olefin function in the protostane structure of **11** were characterized by an HMBC experiment. Namely, long-range correlations were observed between the following protons and carbons: 3-C and 2-H<sub>2</sub>, 27-H<sub>3</sub>, 28-H<sub>3</sub>; 13-C and 12-H<sub>2</sub>, 18-H<sub>3</sub>; 17-C and 16-H<sub>2</sub>, 20-H, 21-H<sub>3</sub>, 28-H<sub>3</sub> (Fig. 1 B). The stereostructure of **11** was characterized from an NOESY experiment as depicted in Fig. 2 b and by comparison of the <sup>1</sup>H-<sup>1</sup>H coupling pattern of the 23 and 24-protons in the <sup>1</sup>H-NMR spectrum of **11** with those for known protostane-type triterpenes having the 24,25-epoxide function.<sup>5-7,9)</sup> Consequently, the structure of alisol I (**11**) was elucidated as shown.

The IR spectra of alisols J-23-acetate (**12**) and K-23-acetate (**13**) were similar and showed absorption bands due to ester, ketone, and enone functions. In the UV spectrum of **12**, an absorption maximum was observed at 246 nm (log  $\epsilon$  3.8), which suggested the presence of an enone function. Alisols J-23-acetate (**12**) and K-23-acetate (**13**) were formed to have the same molecular formula C<sub>32</sub>H<sub>46</sub>O<sub>6</sub>, which was obtained from the positive- and negative-ion FAB-MS [quasimolecular ion peak  $m/z$ : 527 (M+H)<sup>+</sup>, 549 (M+Na)<sup>+</sup>, 525 (M-H)<sup>-</sup>] and by high-resolution MS measurement. The <sup>1</sup>H-NMR (CDCl<sub>3</sub>) and <sup>13</sup>C-NMR (Table 1) spectra of **12**<sup>8)</sup> showed sig-

nals assignable to a trisubstituted olefin [ $\delta$  5.84 (s, 12-H)], a methine bearing an acetoxy group [ $\delta$  2.08 (s, 23-OAc), 4.86 (ddd,  $J=2.8, 8.6, 15.0$  Hz, 23-H)], and two methines bearing an oxygen function [ $\delta$  3.67 (d-like, 16-H), 2.78 (d,  $J=8.6$  Hz, 24-H)] together with seven tertiary methyls, a secondary methyl, and two ketocarbonyl carbons. The plane structure of **12** including the positions of a ketone, an enone, two epoxides, and an acetoxy function was confirmed by an HMBC experiment as shown in Fig. 1 C. The <sup>1</sup>H-NMR (CDCl<sub>3</sub>) and <sup>13</sup>C-NMR (Table 1) spectra of **13**,<sup>8)</sup> in contrast, showed the presence of the same functional groups as **12** and also, in the HMBC experiment on **13** (Fig. 1 C), the same long-range correlations as **12** were observed. This evidence confirmed for us that **12** and **13** were stereoisomers at the 16,17-epoxide moiety. The stereostructures of the 16,17-epoxide in **12** and **13** were clarified by NOESY experiments, which showed NOE correlations between the following protons [**12**: 16-H and 15 $\beta$ -H, 21-H<sub>3</sub>; 15 $\alpha$ -H and 30-H<sub>3</sub>; 23-H and 26-H<sub>3</sub>; 24-H and 27-H<sub>3</sub> (Fig. 2 c). **13**: 16-H and 15 $\alpha$ -H; 15 $\alpha$ -H and 30-H; 23-H and 26-H<sub>3</sub>; 24-H and 27-H<sub>3</sub> (Fig. 2 d)]. The proton and carbon signals of the side chain moiety (C-20—C-27) were found to be very similar to those of known protostane-type triterpenes (ex. **4**, **6**, **8**) having the 23 $\beta$ -acetoxy and the 24 $\beta$ ,25-epoxyl function. On the basis of the above evidence,

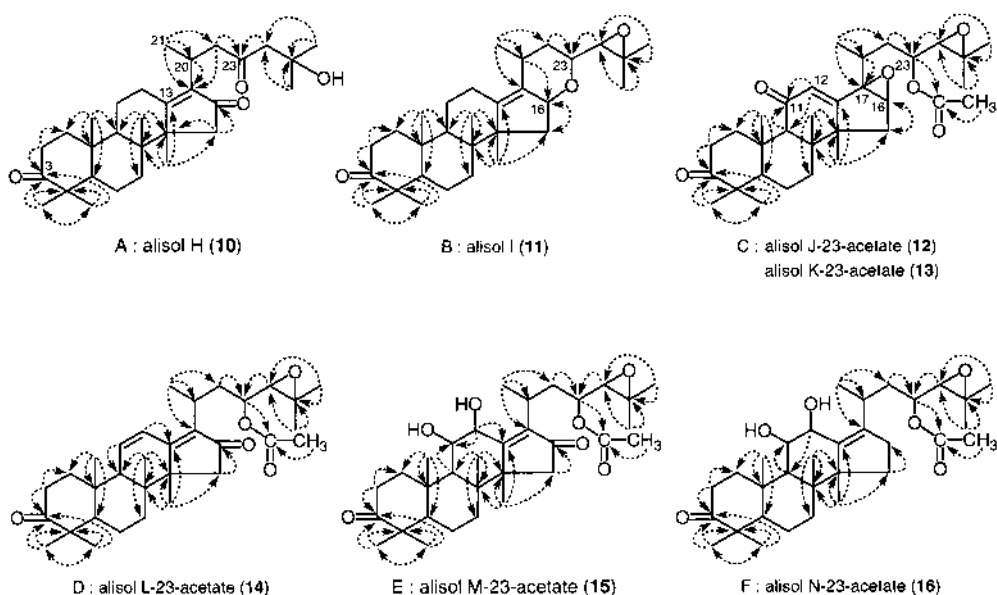


Fig. 1. Long-Range Correlations in the HMBC Spectra of **10**–**16**

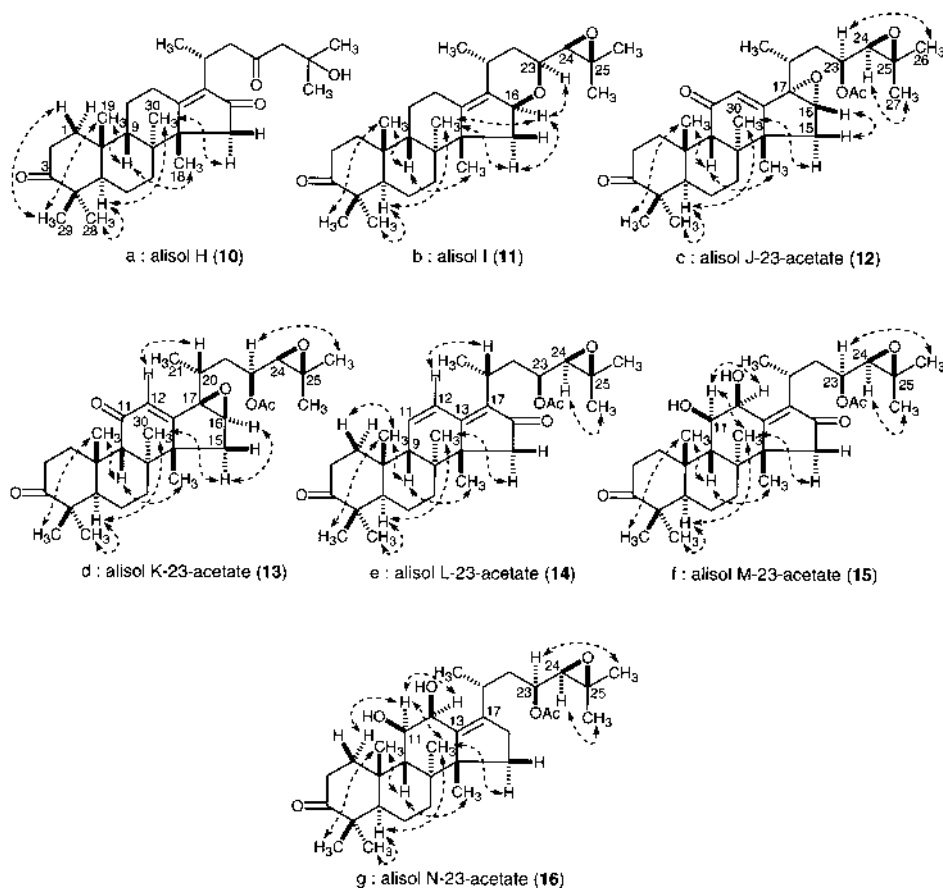


Fig. 2. NOE Correlations in the NOESY Spectra of **10**–**16**

the structures of alisol J-23-acetate (**12**) and alisol K-23-acetate (**13**) were characterized as shown.

Alisol L-23-acetate (**14**) showed absorption bands due to acetyl, ketone, and enone functions in the IR spectrum, while its UV spectrum showed absorption maximum at 285 nm ( $\log \epsilon$  3.4) suggestive of a dienone function. In the positive- and negative-ion FAB-MS of **14**, quasimolecular ion peaks were observed at  $m/z$  511 ( $M+H$ )<sup>+</sup>, 533 ( $H+Na$ )<sup>+</sup>, and 509

( $M-H$ )<sup>-</sup> and the molecular formula  $C_{32}H_{46}O_5$  of **14** was clarified by the high-resolution MS measurement. The <sup>1</sup>H-NMR ( $CDCl_3$ ) and <sup>13</sup>C-NMR (Table 1) spectra of **14**<sup>8)</sup> showed signals assignable to a dienone [ $\delta$  6.48 (dd,  $J=3.7$ , 10.4 Hz, 11-H), 6.14 (dd,  $J=1.8$ , 10.4 Hz, 12-H)], a methine bearing an acetoxy group [ $\delta$  2.06, (s, 23-OAc), 4.57 (ddd,  $J=2.8$ , 8.3, 11.3 Hz, 23-H)], a methine bearing an oxygen function [ $\delta$  2.73 (d,  $J=8.3$  Hz, 24-H)], and an isolated meth-

Table 1.  $^{13}\text{C}$ -NMR Data of Alisols H (**10**), I (**11**), J-23-Acetate (**12**), K-23-Acetate (**13**), L-23-Acetate (**14**), M-23-Acetate (**15**), and N-23-Acetate (**16**) ( $\text{CDCl}_3$ , 125 MHz)

	10	11	12	13	14	15	16
C-1	31.7	31.6	32.3	32.5	32.3	30.8	31.0
C-2	33.6	33.7	33.7	33.7	33.3	33.7	33.8
C-3	219.5	220.1	219.5	219.3	219.1	219.6	220.2
C-4	47.0	47.0	47.0	47.0	47.2	46.9	47.0
C-5	48.0	47.8	48.0	48.3	46.1	48.8	48.9
C-6	19.9	20.0	19.7	20.1	19.3	20.0	20.2
C-7	34.6	33.7	32.9	33.4	31.2	34.7	34.0
C-8	40.4	40.8	41.5	44.7	47.7	40.2	41.3
C-9	42.8	43.9	55.7	55.2	47.7	44.4	45.9
C-10	36.2	36.3	37.1	37.2	36.0	36.7	36.8
C-11	22.1	23.0	199.5	199.5	121.6	70.7	71.2
C-12	24.5	22.4	123.3	124.7	138.5	66.4	66.4
C-13	179.2	139.6	167.1	167.1	171.5	175.8	141.4
C-14	50.0	55.3	56.8	50.2	39.3	49.2	56.9
C-15	45.8	40.0	36.0	33.2	44.6	46.7	31.3
C-16	208.3	79.8	64.0	63.2	207.6	208.6	29.1
C-17	138.8	131.7	70.7	69.4	137.7	140.1	140.4
C-18	22.9	24.4	25.5	25.3	23.8	25.2	26.5
C-19	23.7	23.5	25.1	25.1	24.8	25.5	25.5
C-20	25.8	26.6	28.8	26.9	26.1	27.4	28.1
C-21	19.3	18.4	15.4	18.3	19.8	20.2	20.6
C-22	48.2	34.9	35.8	34.4	35.7	35.9	37.5
C-23	212.6	72.5	71.9	72.0	71.9	73.8	72.5
C-24	53.4	65.7	64.6	64.9	65.0	64.3	64.5
C-25	69.6	57.1	59.2	59.1	58.6	59.0	59.0
C-26	29.2 <sup>a)</sup>	19.3	19.8	19.7	19.4	19.1	19.2
C-27	29.3 <sup>a)</sup>	25.0	24.6	24.7	24.7	24.6	24.7
C-28	29.4	29.3	29.4	29.4	29.3	29.6	29.1
C-29	19.7	19.7	19.4	19.4	19.2	20.1	20.2
C-30	22.0	22.7	24.9	24.7	21.9	22.9	23.7
Ac-1			170.3	170.3	170.0	173.1	172.6
Ac-2			21.2	21.2	21.1	21.4	21.3

a) May be interchangeable.

ylene adjacent to a carbonyl function [ $\delta$  1.90, 2.36 (both d,  $J=18.3$  Hz, 15- $\text{H}_2$ )] together with methyls and methylenes due to protostane-type triterpene skeleton. The plane structure of **14** was determined by an HMBC experiment, which showed long-range correlations between the following protons and carbons: 3-C and 2- $\text{H}_2$ , 28- $\text{H}_3$ , 29- $\text{H}_3$ ; 9-C and 11-H, 30- $\text{H}_3$ ; 13-C and 12-H; 16-C and 15- $\text{H}_2$ ; 17-C and 21- $\text{H}_3$ ; 24-C and 23-H, 26- $\text{H}_3$ , 27- $\text{H}_3$ ; 25-C and 26- $\text{H}_3$ , 27- $\text{H}_3$ ; acetyl carbonyl-C and 23-H, acetyl- $\text{H}_3$  (Fig. 1 D). The carbon signals in the  $^{13}\text{C}$ -NMR spectrum of **14** were very similar to those of **8**, except for the signals due to the disubstituted olefin of the C-ring part in **14**. The stereostructure of **14** was deduced by a NOESY experiment, and the stereostructure of the side chain bonded to the 17-position was deduced to be the same as that of **4**, **6**, and **8** by comparison of the  $^1\text{H}$ - and  $^{13}\text{C}$ -NMR data. Consequently, the structure of alisol L-23-acetate (**14**) was elucidated as shown.

The IR spectrum of alisol M-23-acetate (**15**) showed absorption bands at 3480, 1738, 1705, and 1695  $\text{cm}^{-1}$  assignable to hydroxyl, acetyl, ketone, and enone functions, whereas an absorption maximum was observed at 244 nm ( $\log \epsilon$  3.8) in its UV spectrum. Here again, the molecular formula  $\text{C}_{32}\text{H}_{48}\text{O}_7$  was determined from the positive- and negative-ion FAB-MS [ $m/z$  545 ( $\text{M}+\text{H}$ ) $^+$ , 567 ( $\text{M}+\text{Na}$ ) $^+$ , 543 ( $\text{M}-\text{H}$ ) $^+$ ] and by high-resolution MS measurement. The  $^1\text{H}$ -NMR ( $\text{CDCl}_3$ ) and  $^{13}\text{C}$ -NMR (Table 1) spectra of **15**<sup>8)</sup> showed the presence of two methines bearing a hydroxyl group [ $\delta$  3.86

(m, 11-H), 4.53 (br s, 12-H)], a methine bearing an acetoxy group [ $\delta$  2.16 (s, 23-OAc), 4.57 (ddd,  $J=2.2, 8.9, 11.0$  Hz, 23-H)], an epoxide [ $\delta$  2.82 (d,  $J=8.9$  Hz, 24-H)], and an isolated methylene adjacent to a ketocarbonyl function [ $\delta$  1.80, 2.47 (both d,  $J=19.2$  Hz, 15- $\text{H}_2$ )]. The plane structure of **15** was also determined from an HMBC experiment (Fig. 1 E) and its stereostructure including the vicinal diol moiety was clarified by a NOESY experiment, which showed NOE correlations between the 11-proton and the 12-proton and between the 11-proton and the 30-methyl protons (Fig. 2 f). This evidence and comparison of the  $^1\text{H}$ - and  $^{13}\text{C}$ -NMR data for **15** with those of known protostane-type triterpenes such as **8** and **14** led us to formulate the structure of alisol M-23-acetate (**15**) as shown.

Alisol N-23-acetate (**16**) showed absorption bands due to hydroxyl, ester, and ketone functions. The molecular formula  $\text{C}_{32}\text{H}_{50}\text{O}_6$  was determined from the positive- and negative-ion FAB-MS [ $m/z$  531 ( $\text{M}+\text{H}$ ) $^+$ , 553 ( $\text{M}+\text{Na}$ ) $^+$ , 529 ( $\text{M}-\text{H}$ ) $^-$ ] and by high-resolution FAB-MS measurement. The  $^1\text{H}$ -NMR ( $\text{CDCl}_3$ ) and  $^{13}\text{C}$ -NMR (Table 1) spectra of **16**<sup>8)</sup> showed the presence of a vicinal diol moiety [ $\delta$  3.73 (m, 11-H), 4.35 (br s, 12-H)], a methine bearing an acetoxy group [ $\delta$  2.14 (s, 23-OAc), 4.75 (ddd-like, 23-H)], and an epoxide [ $\delta$  2.80 (d,  $J=8.6$  Hz, 24-H)]. The carbon signals in the  $^{13}\text{C}$ -NMR spectrum of **16** were superimposable on those of **15**, except for the signals due to the carbons on D-ring. The plane structure of **16** was determined by an HMBC experiment (Fig. 1 F) and its stereostructure was deduced by a NOESY experiment (Fig. 2 g). On the basis of the above evidence and comparison of the  $^1\text{H}$ - and  $^{13}\text{C}$ -NMR data for **16** with those for **4**, the structure of alisol N-23-acetate (**16**) was elucidated as shown.

## Experimental

The following instruments were used to obtain physical data: melting points, Yanagimoto micro-melting point apparatus MP-500D (values are uncorrected); specific rotations, Horiba SEPA-300 digital polarimeter ( $l=5$  cm); UV spectra, Shimadzu UV-1200 spectrometer; IR spectra, Shimadzu FTIR-8100 spectrometer; EI-MS and high-resolution MS, JEOL JMS-GC-MATE mass spectrometer; FAB-MS and high-resolution MS, JEOL JMS-SX 102A mass spectrometer;  $^1\text{H}$ -NMR spectra, JNM-LA500 (500 MHz) spectrometer;  $^{13}\text{C}$ -NMR spectra, JNM-LA500 (125 MHz) spectrometer with tetramethylsilane as an internal standard.

The following experimental conditions were used for chromatography: ordinary-phase silica gel column chromatography, Silica gel BW-200 (Fuji Silysia Chemical, Ltd., 150–350 mesh); reversed-phase silica gel column chromatography, Chromatorex ODS DM1020T (Fuji Silysia Chemical, Ltd., 100–200 mesh); TLC, pre-coated TLC plates with Silica gel 60F<sub>254</sub> (Merck, 0.25 mm) (ordinary phase) and Silica gel RP-18 60F<sub>254</sub> (Merck, 0.25 mm) (reversed phase); reversed-phase HPTLC, pre-coated TLC plates with Silica gel RP-18 60WF<sub>254S</sub> (Merck, 0.25 mm); detection was achieved by spraying with 1%  $\text{Ce}(\text{SO}_4)_2$ -10% aqueous  $\text{H}_2\text{SO}_4$  and heating.

**Isolation of Protostane-Type Triterpenes from the Dried Rhizome of *Alisma orientale*** The MeOH extract (1.5 kg) from Chinese *Alismatis Rhizoma* (20 kg) was partitioned into a mixture of AcOEt–water. Isolation of major constituents, alismol, alismoxide, alisols A (**1**) and B (**3**) and their monoacetate (**2**, **4**), from the AcOEt-soluble portion was reported previously.<sup>2)</sup> The AcOEt-soluble portion (300 g) was subjected to silica gel column chromatography [BW-200 (Fuji Silysia Chemical, Ltd., 3 kg),  $\text{CHCl}_3$ -MeOH (50:1→30:1→10:1)→MeOH] to give nine fractions [fr. 1 (29.8 g), fr. 2 (38.7 g), fr. 3 (55.3 g), fr. 4 (60.6 g), fr. 5 (23.2 g), fr. 6 (25.6 g), fr. 7 (20.1 g), fr. 8 (10.3 g), fr. 9 (36.4 g)]. Fraction 2 (38.7 g) was further separated by repeated silica gel column [1.5 kg each, 1) *n*-hexane–acetone (10:1→4:1→2:1)→ $\text{CHCl}_3$ -acetone (10:1); 2)  $\text{CHCl}_3$ -acetone (30:1→5:1)→ $\text{CHCl}_3$ ], ODS column [Chromatorex ODS DM 1020T (Fuji Silysia Chemical, Ltd.), MeOH- $\text{H}_2\text{O}$ ], and finally HPLC [column: YMC-Pack R&D-ODS-5-A, 250×20 mm i.d., solvent: 80–90% aqueous MeOH, flow

rate: 9.0—10.0 ml/min] to furnish isolis H (**10**, 18.2 mg), I (**11**, 41.5 mg), J-23-acetate (**12**, 52.5 mg), K-23-acetate (**13**, 52.4 mg), L-23-acetate (**14**, 27.3 mg), M-23-acetate (**15**, 28.4 mg), and N-23-acetate (**16**, 19.7 mg) and 11-deoxyisolis B (**5**, 15 mg), B-23-acetate (**6**, 139 mg), C (**7**, 9 mg), and C-monoacetate (**8**, 115 mg). Known protostane-type triterpenes were identified by comparison with authentic samples ( $^1\text{H}$ - and  $^{13}\text{C}$ -NMR, IR, and  $[\alpha]_D^{25}$  data).

Alisol H (**10**): A white powder,  $[\alpha]_D^{25} + 59.1^\circ$  ( $c=0.9$ ,  $\text{CHCl}_3$ ). High-resolution negative-ion FAB-MS: Calcd for  $\text{C}_{30}\text{H}_{47}\text{O}_4$  ( $\text{M}+\text{H}$ ) $^+$ : 471.3474. Found: 471.3488. UV  $\lambda_{\text{max}}^{\text{CHCl}_3}$  nm (log  $\epsilon$ ): 243 (3.8). IR (KBr): 3481, 1705, 1700, 1665, 1462, 1379, 1238  $\text{cm}^{-1}$ .  $^1\text{H}$ -NMR ( $\text{CDCl}_3$ )  $\delta$ : 0.88, 0.92, 1.06, 1.07, 1.18, 1.20, 1.24 (3H each, all s, 19, 30, 29, 28, 26, 27, 18- $\text{H}_3$ ), 1.16 (3H, d,  $J=7.0$  Hz, 21- $\text{H}_3$ ), 1.49, 2.07 (1H each, both m, 1- $\text{H}_2$ ), 1.80, 2.44 (1H each, both d,  $J=19.5$  Hz, 15- $\text{H}_2$ ), 1.83 (1H, s, 9-H), 1.98 (1H, m, 5-H), 2.30, 2.64 (1H each, both m, 2- $\text{H}_2$ ), 2.52, 2.54 (1H each, both d,  $J=20.3$  Hz, 24- $\text{H}_2$ ), 2.66, 2.98 (1H each, both m, 22- $\text{H}_2$ ).  $^{13}\text{C}$ -NMR ( $\text{CDCl}_3$ )  $\delta_{\text{C}}$ : Given in Table 1. Positive-ion FAB-MS  $m/z$ : 471 ( $\text{M}+\text{H}$ ) $^+$ , 493 ( $\text{M}+\text{Na}$ ) $^+$ . Negative-ion FAB-MS  $m/z$  469: ( $\text{M}-\text{H}$ ) $^-$ .

Alisol I (**11**): A white powder,  $[\alpha]_D^{25} + 51.9^\circ$  ( $c=2.1$ ,  $\text{CHCl}_3$ ). High-resolution EI-MS: Calcd for  $\text{C}_{30}\text{H}_{46}\text{O}_3$  ( $\text{M}^+$ ): 454.3447. Found: 454.3422. IR (KBr): 1705, 1458, 1377, 1242  $\text{cm}^{-1}$ .  $^1\text{H}$ -NMR ( $\text{CDCl}_3$ )  $\delta$ : 0.82, 0.91, 1.03, 1.06, 1.20 (3H each, all s, 19, 30, 29, 28, 18- $\text{H}_3$ ), 1.15 (3H, d,  $J=7.8$  Hz, 21- $\text{H}_3$ ), 1.31 (6H, s, 26, 27- $\text{H}_3$ ), 1.33, 2.30 (1H each, both m, 15- $\text{H}_2$ ), 1.42, 2.03 (1H each, both m, 1- $\text{H}_2$ ), 1.68 (1H, dd-like, 9-H), 2.03 (1H, m, 5-H), 2.30, 2.63 (1H each, both m, 2- $\text{H}_2$ ), 2.71 (1H, d,  $J=7.9$  Hz, 24-H), 3.53 (1H, ddd,  $J=2.1, 7.9, 12.2$  Hz, 23-H), 4.47 (1H, dd-like, 16-H).  $^{13}\text{C}$ -NMR ( $\text{CDCl}_3$ )  $\delta_{\text{C}}$ : Given in Table 1. EI-MS  $m/z$ : 454 ( $\text{M}^+$ ).

Alisol J-23-Acetate (**12**): A white powder,  $[\alpha]_D^{25} + 39.1^\circ$  ( $c=2.6$ ,  $\text{CHCl}_3$ ). High-resolution positive-ion FAB-MS: Calcd for  $\text{C}_{32}\text{H}_{47}\text{O}_6$  ( $\text{M}+\text{H}$ ) $^+$ : 527.3373. Found: 527.3386. UV  $\lambda_{\text{max}}^{\text{CHCl}_3}$  nm (log  $\epsilon$ ): 246 (3.8). IR (KBr): 1738, 1700, 1661, 1462, 1382, 1238  $\text{cm}^{-1}$ .  $^1\text{H}$ -NMR ( $\text{CDCl}_3$ )  $\delta$ : 1.04 (3H, d,  $J=7.0$  Hz, 21- $\text{H}_3$ ), 1.05, 1.08, 1.10, 1.17, 1.33, 1.36, 1.38 (3H each, all s, 29, 28, 25, 30, 18, 26, 27- $\text{H}_3$ ), 1.56, 1.58 (1H each, both d,  $J=3.4$  Hz, 15- $\text{H}_2$ ), 1.92, 2.44 (1H each, both m, 1- $\text{H}_2$ ), 2.08 (3H, s, 23-OAc), 2.22 (1H, m, 5-H), 2.37, 2.68 (1H each, both m, 2- $\text{H}_2$ ), 2.58 (1H, m, 9-H), 2.78 (1H, d,  $J=8.6$  Hz, 24-H), 3.67 (1H, d-like, 16-H), 4.86 (1H, ddd,  $J=2.8, 8.6, 15.0$  Hz, 23-H), 5.84 (1H, s, 12-H).  $^{13}\text{C}$ -NMR ( $\text{CDCl}_3$ )  $\delta_{\text{C}}$ : Given in Table 1. Positive-ion FAB-MS  $m/z$ : 527 ( $\text{M}+\text{H}$ ) $^+$ , 549 ( $\text{M}+\text{Na}$ ) $^+$ . Negative-ion FAB-MS  $m/z$ : 525 ( $\text{M}-\text{H}$ ) $^-$ .

Alisol K-23-Acetate (**13**): A white powder,  $[\alpha]_D^{25} + 69.4^\circ$  ( $c=2.6$ ,  $\text{CHCl}_3$ ). High-resolution positive-ion FAB-MS: Calcd for  $\text{C}_{32}\text{H}_{47}\text{O}_6$  ( $\text{M}+\text{H}$ ) $^+$ : 527.3372. Found: 527.3386. IR (KBr): 1738, 1705, 1661, 1460, 1379, 1240  $\text{cm}^{-1}$ .  $^1\text{H}$ -NMR ( $\text{CDCl}_3$ )  $\delta$ : 1.05, 1.08, 1.11, 1.17, 1.33, 1.34, 1.37 (3H each, all s, 29, 28, 19, 30, 27, 18, 26- $\text{H}_3$ ), 1.07 (3H, d,  $J=7.0$  Hz, 21- $\text{H}_3$ ), 1.74, 2.02 (1H each, both dd-like, 15- $\text{H}_2$ ), 1.91, 2.45 (1H each, both m, 1- $\text{H}_2$ ), 2.09 (3H, s, 23-OAc), 2.15 (1H, m, 5-H), 2.30, 2.68 (1H each, both m, 2- $\text{H}_2$ ), 2.66 (1H, s, 9-H), 2.78 (1H, d,  $J=8.5$  Hz, 24-H), 3.67 (1H, d,  $J=1.9$  Hz, 16-H), 4.89 (1H, ddd,  $J=2.5, 8.5, 13.8$  Hz, 23-H), 5.91 (1H, s, 12-H).  $^{13}\text{C}$ -NMR ( $\text{CDCl}_3$ )  $\delta_{\text{C}}$ : Given in Table 1. Positive-ion FAB-MS  $m/z$ : 527 ( $\text{M}+\text{H}$ ) $^+$ , 549 ( $\text{M}+\text{Na}$ ) $^+$ . Negative-ion FAB-MS  $m/z$ : 525 ( $\text{M}-\text{H}$ ) $^-$ .

Alisol L-23-Acetate (**14**): A white powder,  $[\alpha]_D^{25} + 86.7^\circ$  ( $c=1.4$ ,  $\text{CHCl}_3$ ). High-resolution FAB-MS: Calcd for  $\text{C}_{32}\text{H}_{47}\text{O}_5$  ( $\text{M}+\text{H}$ ) $^+$ : 511.3424. Found: 511.3430. UV  $\lambda_{\text{max}}^{\text{CHCl}_3}$  nm (log  $\epsilon$ ): 285 (3.4). IR (KBr): 1740, 1705, 1665, 1458, 1379, 1285  $\text{cm}^{-1}$ .  $^1\text{H}$ -NMR ( $\text{CDCl}_3$ )  $\delta$ : 0.94, 0.96, 1.06, 1.09, 1.12, 1.27, 1.30 (3H each, all s, 19, 30, 29, 28, 18, 26, 27- $\text{H}_3$ ), 1.17 (3H, d,  $J=7.0$  Hz, 21- $\text{H}_3$ ), 1.68, 2.06 (1H each, both m, 1- $\text{H}_2$ ), 1.90, 2.36 (1H each, both d,  $J=18.3$  Hz, 15- $\text{H}_2$ ), 2.06 (3H, s, 23-OAc), 2.28, 2.71 (1H each, both m, 2-

$\text{H}_2$ ), 2.32 (1H, m, 5-H), 2.38 (1H, s, 9-H), 2.73 (1H, d,  $J=8.3$  Hz, 24-H), 4.57 (1H, ddd,  $J=2.8, 8.3, 11.3$  Hz, 23-H), 6.14 (1H, dd,  $J=1.8, 10.4$  Hz, 12-H), 6.48 (1H, dd,  $J=3.7, 10.4$  Hz, 11-H).  $^{13}\text{C}$ -NMR ( $\text{CDCl}_3$ )  $\delta_{\text{C}}$ : Given in Table 1. Positive-ion FAB-MS  $m/z$ : 511 ( $\text{M}+\text{H}$ ) $^+$ , 533 ( $\text{M}+\text{Na}$ ) $^+$ . Negative-ion FAB-MS  $m/z$ : 509 ( $\text{M}-\text{H}$ ) $^-$ .

Alisol M-23-Acetate (**15**): A white powder,  $[\alpha]_D^{25} + 35.4^\circ$  ( $c=1.4$ ,  $\text{CHCl}_3$ ). High-resolution positive-ion FAB-MS: Calcd for  $\text{C}_{32}\text{H}_{49}\text{O}_7$  ( $\text{M}+\text{H}$ ) $^+$ : 545.3479. Found: 545.3477.  $\lambda_{\text{max}}^{\text{CHCl}_3}$  nm (log  $\epsilon$ ): 244 (3.8). IR (KBr): 3480, 1738, 1705, 1675, 1462, 1381, 1238  $\text{cm}^{-1}$ .  $^1\text{H}$ -NMR ( $\text{CDCl}_3$ )  $\delta$ : 0.88, 1.08, 1.09, 1.10, 1.17, 1.31, 1.48 (3H each, all s, 30, 29, 28, 19, 26, 27, 18- $\text{H}_3$ ), 1.16 (3H, d,  $J=6.2$  Hz, 21- $\text{H}_3$ ), 1.80, 2.47 (1H each, both d,  $J=19.2$  Hz, 15- $\text{H}_2$ ), 2.05 (1H, m, 5-H), 2.08 (1H, m, 9-H), 2.16 (3H, s, 23-OAc), 2.24 (2H, m, 1- $\text{H}_2$ ), 2.38, 2.65 (1H each, both m, 2- $\text{H}_2$ ), 2.82 (1H, d,  $J=8.9$  Hz, 24-H), 3.86 (1H, m, 11-H), 4.53 (1H, br s, 12-H), 4.57 (1H, ddd,  $J=2.2, 8.9, 11.0$  Hz, 23-H).  $^{13}\text{C}$ -NMR ( $\text{CDCl}_3$ )  $\delta_{\text{C}}$ : Given in Table 1. Positive-ion FAB-MS  $m/z$ : 545 ( $\text{M}+\text{H}$ ) $^+$ , 567 ( $\text{M}+\text{Na}$ ) $^+$ . Negative-ion FAB-MS  $m/z$ : 543 ( $\text{M}-\text{H}$ ) $^-$ .

Alisol N-23-Acetate (**16**): A white powder,  $[\alpha]_D^{25} + 52.9^\circ$  ( $c=1.0$ ,  $\text{CHCl}_3$ ). High-resolution positive-ion FAB-MS: Calcd for  $\text{C}_{32}\text{H}_{51}\text{O}_6$  ( $\text{M}+\text{H}$ ) $^+$ : 531.3686. Found: 531.3678. IR (KBr): 3503, 1739, 1705, 1462, 1377, 1242  $\text{cm}^{-1}$ .  $^1\text{H}$ -NMR ( $\text{CDCl}_3$ )  $\delta$ : 0.95, 1.05, 1.06, 1.07, 1.31, 1.32, 1.33 (3H each, all s, 30, 19, 28, 29, 18, 26, 27- $\text{H}_3$ ), 1.01 (3H, d,  $J=9.2$  Hz, 21- $\text{H}_3$ ), 1.28, 1.93 (1H each, both m, 15- $\text{H}_2$ ), 1.98 (1H, m, 9-H), 2.03 (1H, m, 5-H), 2.10, 2.22 (1H each, both m, 16- $\text{H}_2$ ), 2.14 (3H, s, 23-OAc), 2.22 (2H, m, 1- $\text{H}_2$ ), 2.37, 2.63 (1H each, both m, 2- $\text{H}_2$ ), 2.80 (1H, d,  $J=8.6$  Hz, 24-H), 3.73 (1H, m, 11-H), 4.35 (1H, br s, 12-H), 4.75 (1H, ddd-like, 23-H).  $^{13}\text{C}$ -NMR ( $\text{CDCl}_3$ )  $\delta_{\text{C}}$ : given in Table 1. Positive-ion FAB-MS  $m/z$ : 531 ( $\text{M}+\text{H}$ ) $^+$ , 553 ( $\text{M}+\text{Na}$ ) $^+$ . Negative-ion FAB-MS  $m/z$ : 529 ( $\text{M}-\text{H}$ ) $^-$ .

## References and Notes

- Matsuda H., Tomohiro N., Yoshikawa M., Kubo M., *Biol. Pharm. Bull.*, **21**, 1317—1321 (1998).
- Kubo M., Matsuda H., Tomohiro N., Yoshikawa M., *Biol. Pharm. Bull.*, **20**, 511—516 (1997).
- a) Murata T., Imai Y., Hirata T., Miyamoto M., *Chem. Pharm. Bull.*, **18**, 1347—1353 (1970); b) Murata T., Miyamoto M., *ibid.*, **18**, 1354—1361 (1970); c) Kamiya K., Murata T., Nishikawa M., *ibid.*, **18**, 1362—1368 (1970); d) Murata T., Shinohara M., Miyamoto M., *ibid.*, **18**, 1369—1384 (1970).
- a) Yoshikawa M., Hatakeyama S., Tanaka N., Fukuda Y., Murakami N., Yamahara J., *Chem. Pharm. Bull.*, **40**, 2582—2584 (1992); b) Yoshikawa M., Yamaguchi S., Matsuda H., Kohda Y., Ishikawa H., Tanaka N., Yamahara J., Murakami N., *ibid.*, **42**, 1813—1816 (1994).
- Yoshikawa M., Hatakeyama S., Tanaka N., Matsuoka T., Yamahara J., Murakami N., *Chem. Pharm. Bull.*, **41**, 2109—2112 (1993).
- Pei W. G., Fukuyama Y., Yamada T., Rei W., Jinxian B., Nakagawa K., *Phytochemistry*, **27**, 1161—1164 (1988).
- Nakajima Y., Satoh Y., Katsumata M., Tsujiyama K., Ida Y., Shoji J., *Phytochemistry*, **36**, 119—127 (1994).
- The  $^1\text{H}$ - and  $^{13}\text{C}$ -NMR data of **10**—**16** were assigned with the aid of homo- and hetero-correlation spectroscopy ( $^1\text{H}$ - $^1\text{H}$ ,  $^1\text{H}$ - $^{13}\text{C}$  COSY), homo- and hetero-nuclear Hartmann-Hahn spectroscopy ( $^1\text{H}$ - $^1\text{H}$ ,  $^1\text{H}$ - $^{13}\text{C}$  HOHAHA), distortionless enhancement polarization transfer (DEPT), NOESY, and HMBC experiments.
- Yoshikawa M., Hatakeyama S., Tanaka N., Fukuda Y., Yamahara J., Murakami N., *Chem. Pharm. Bull.*, **41**, 1948—1954 (1993).